Physically-based definition of rainfall thresholds for shallow landslides in a tropical mountain watershed of the Colombian Andes.

Roberto J. Marin [1, 2], Álvaro J. Mattos [2] & Jesner Marín-Londoño [2].

[1] *Landslide Scientific Assessment (LandScient), Medellín, Colombia.*

[2] *Environmental School, Faculty of Engineering, University of Antioquia (UdeA). Calle 70 #52-21, Medellín, Colombia.*

rjose.marin@udea.edu.co

Abstract

Landslides cause important impacts around the world, with many human and economic losses. For its prediction, rainfall thresholds have been used to represent the relationship between precipitation and landslide occurrence. Distributed physically-based models have also been used to define thresholds for shallow landslides based on the variation of the factor of safety (FS) due to rainfall infiltration. In this work, rainfall intensity (I) and duration (D) thresholds are determined in a tropical mountain watershed of Envigado (Colombia) using two physically-based models: TRIGRS and Papa's model. In both cases, multiple simulations were made to determine the critical rainfall intensity and duration conditions that cause instability in a percentage of the total area (a_c) of the study site and to compare the characteristics of the threshold curves of both models. These critical I-D conditions were fitted to power-law equations and a comparison was made between the curves obtained using different a_c values. The rainfall thresholds determined with both models presented a good fitting to a power-law equation, but Papa's model had a higher correlation ($R^2 > 0.99$) for the different ac values that were implemented.

1 INTRODUCTION

Almost all around the world, landslides cause significant impacts reflected in casualties and economic losses (Corominas et al., 2014). They are usually investigated focusing on hydrologic processes and their influence on soil mechanical properties, possibly because the rainfall is the most common cause of its occurrence (Sidle & Bogaard, 2016). Nevertheless, other conditioning factors take importance in the study of this phenomenon (e.g. slope angle, soil properties, groundwater level) (Fell et al., 2008), and even some authors have focused on the effect of other internal factors such as the bedrock topography (Lanni, McDonnell, Hopp, & Rigon, 2013; Moradi, Huisman, Class, & Vereecken, 2018), soil depth (Ho, Lee, Chang, Wang, & Liao, 2012), or vegetation (Kim, Im, Lee, & Woo, 2013; Marín & Osorio, 2017a).

Colombia is one of the countries of the world that is most affected by the occurrence of landslides (Aristizábal & Sánchez, 2019). The Valle de Aburrá region of Colombia, located in the intertropical zone, has great variability in the annual rainfall and is constantly affected by extreme events so that this mountainous region is especially prone to the occurrence of shallow landslides and debris flows (Marín, 2017).

For its prediction, the definition of rainfall thresholds has been considered as an efficient approach to study the relationship between precipitation and landslides (Zhao et al., 2019). The shallow landslides assessment can be carried out considering information on hydrological processes such as rainfall-runoff, infiltration, pore pressure changes, and precipitation. An analysis of these processes can be coupled to spatially distributed slope stability models (e.g. Aristizábal, Vélez, Martínez, & Jaboyedoff, 2016; Montgomery & Dietrich, 1994; Montrasio & Valentino, 2008) for landslide assessment, with different applications found in the scientific literature: landslide susceptibility (Marín & Osorio, 2016; Park, Jang, & Lee, 2019), landslide hazard (Balzano et al., 2019; García-Aristizábal, Aristizabal, Marín, & Guzman-Martinez, 2019), landslide risk (Ip, Rahardjo, & Satyanaga, 2020; Marín, Marín-Londoño, & Mattos, 2020; Marín et al., 2018), and rainfall threshold definition (Marin & Velásquez, 2020; Zhang et al., 2020).

In distributed physically-based models the factor of safety (FS) constitutes a margin against slope failure (FS < 1.0). During a rainfall event, the value of FS decreases as the infiltration of the water in the soil increases (Hsu et al., 2018). Some distributed physical models such as TRIGRS (Baum, Savage, & Godt, 2008) and Papa, Medina, Ciervo, & Bateman (2013) use infinite slope stability analysis to calculate the factor of safety, using different hydrologic assumptions.

Rainfall thresholds are commonly defined using statistical-empirical methodologies that require sufficient data (landslide inventories) that are not always available. Also, its applicability in small areas (local or at a basin scale) generally is not possible or could have very low predictive accuracy (Bogaard & Greco, 2018). Therefore, the definition of rainfall thresholds using physically-based methodologies can be a good option. In this study, a comparison of rainfall intensity and duration thresholds determined using these models in a tropical mountain catchment of Envigado (Colombia) is made, analyzing the adjustment of these thresholds to power-law equations.

This paper is outlined as follows. In the methodology (Section 2), concepts for the study and analysis of rainfall thresholds are presented based on the distributed physically-based models TRIGRS and Papa et al. (2013) and the environmental conditions (e.g., topography, geology) of the study site located in the Colombian Andes are pointed out. In the results (Section 3), a discussion of the most important analyzes associated with the study of rainfall intensity-duration diagrams based on the proportion of the failing area (i.e. unstable grid cells) of the basin is addressed. Finally, conclusions (Section 4) of this research and description of possible future works derived from the results are presented.

2 METHODOLOGY

2.1 TRIGRS model

TRIGRS v2.1 (Alvioli & Baum, 2016) is a Fortran program for modeling the timing and distribution of rainfall-induced shallow landslides. A one-dimensional infinite-slope stability model is implemented, which is derived from the balance of the vertical component of gravity with the resisting stress due to basal Coulomb friction and pore pressure. The factor of safety of the infinite-slope is calculated by the Taylor (1948) equation:

$$FS(Z,t) = \frac{\tan\phi'}{\tan\delta} + \frac{c' - \psi(Z,t)\gamma_w \tan\phi'}{\gamma_s Z \sin\delta\cos\delta}, \quad (1)$$

where c' is the effective cohesion, ϕ' the effective friction angle, γ_w the water unit weight, γ_s the soil unit weight, ψ the head pressure, Z the depth below the ground surface, t the time, and δ the slope angle. Failure is predicted when FS < 1.0 and stability is preserved when FS ≥ 1.

Complementary, the Richards (1931) equation is implemented to simulate the transient infiltration for unsaturated soil conditions. The rainfall infiltration affects the rise of the water table and the subsurface flow is one-dimensional in the vertical direction. The pressure head is calculated as a function of the depth (Z) and the time (t) using a linearized solution of the Richards (1931) equation proposed by Srivastava & Yeh (1991) using the exponential hydraulic model of Gardner (1958). The hydrological model of TRIGRS requires these input parameters: the saturated (θ_s) and residual (θ_r) volumetric water contents, the inverse of the vertical height of the capillary fringe above the water table (α), the saturated hydraulic conductivity (K_s), the saturated hydraulic diffusivity (D_0) and the steady infiltration rate (I_{ZLT}). A more detailed explanation of the theoretical basis and derived formulas of the physical processes (infiltration, subsurface flow, runoff routing) are described in the official manuals and publications (Baum, Savage, & Godt, 2002; Baum et al., 2008; Baum, Godt, & Savage, 2010).

2.2 Papa et al. (2013) model

In Papa et al. (2013) model, the factor of safety is calculated using Taylor's equation, as does the TRIGRS model (Eq. (1)). On the one hand, the pressure head $\psi(Z,t)$ is determined based on Iverson (2000) approach, where the short-term rainfall response is analyzed considering vertical infiltration. Through infinite-slope analysis, the soil is modeled as a single (homogeneous) stratum, without interactions between neighboring cells.

An analytical solution of a linearization of the Richards equation is proposed, which is appropriate in initial conditions nearby to full saturation of the soil. The boundary conditions are zero transient underground vertical flow at great depths below the water table and the entry of water on the ground surface is governed by Darcy's law. Pore pressures that induce instability are calculated as a superposition of the effect of the actual rainfall event and the background (steady) rainfall, where the pressure head $\psi(Z,t)$ is calculated by Eq. (6).

$$\psi(Z,t) = \psi(Z,0) + Z\frac{I_z}{K_s}R(T^*), \quad (6)$$

where t is the rainfall time duration, $\psi(Z,0)$ the initial pressure head, and I_z the infiltration ratio on the ground surface (in the normal direction to the slope). R(T*) is defined by Eq. (7) and (8).

$$R(T^*) = \sqrt{\frac{T^*}{\pi}}\exp\left(-\frac{1}{T^*}\right) - \mathrm{erfc}\left(\frac{1}{T^*}\right), \quad (7)$$

$$T^* = \left(\frac{4D_0 t\cos^2\delta}{Z^2}\right), \quad (8)$$

where D_0 is the hydraulic diffusivity. A more detailed description of this model can be found in Papa et al. (2013).

2.3 Rainfall thresholds

The methodology implemented to calculate the rainfall thresholds in a mountain tropical catchment is based on the methodology proposed by Alvioli et al. (2014). Initially, an unstable basin is defined as the condition in which a critical failure area (a_c) is reached or exceeded. The possible initiation of landslides in a catchment (associated with an I-D rainfall threshold) is related to a percentage of its total area (Δa_f) that presents landslides in a simulation in TRIGRS (initially stable cells that reach the condition of FS < 1.0).

The definition of rainfall thresholds was carried out by executing TRIGRS (v2.1) (Alvioli & Baum, 2016) increasing the rainfall intensity (for a specific duration) until the condition of $\Delta a_f \geq a_c$ was reached. This process was repeated with another duration. The sets of critical I-D were fitted to a power-law equation:

$$I = \alpha D^{\beta} \quad (9)$$

where I is the mean rainfall intensity, D the duration of the rainfall event, α is a scale parameter (intercept), β is a shape parameter which defines the slope of the I-D curve.

Two Python programs were developed to carry out this methodology. One of them uses the TRIGRS software (v2.1), with external executions, and the other incorporates the equations of Papa's model for the calculation of the factor of safety. In both cases, the map of FS is analyzed calculating the percentage of the failing area (Δa_f). When the condition of $\Delta a_f \geq a_c$ is reached, the critical I-D sets of values are plotted together with a potential curve adjusted to these points.

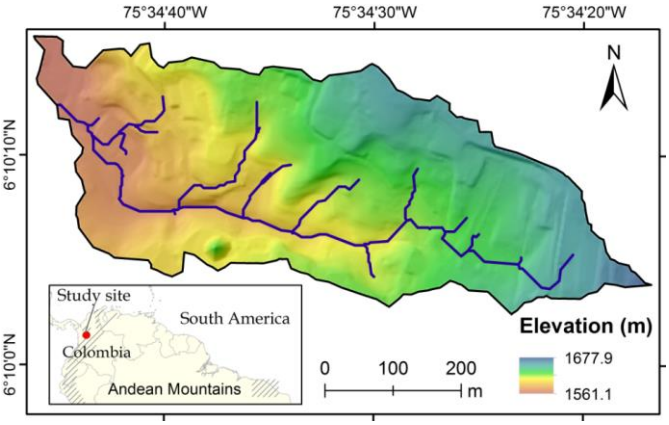

Figure 1. Location of the study area and digital elevation model of the watershed of Envigado, Colombia.

In this study, durations ranging from 1 h to 150 h and rainfall intensities from 1 mm/h to 200 mm/h were used in the simulations. For long durations, the intensities that cause $\Delta a_f \geq a_c$ have little variation, so that the range of durations of the rainfall thresholds is controlled by excluding the critical intensity conditions that are repeated in periods of time greater than 10 h.

2.4 Study site

A small basin located in the Cordillera Central of the Colombian Andes, municipality of Envigado, subregion of the Valle de Aburrá (Antioquia, Colombia), is the study site selected for the application of this methodology. The study site is formed by a mountainous relief with elevation ranging between 1561 and 1678 m, with an average temperature of 22 °C, average annual rainfall of 2170 mm/year and classified in climatic terms as humid tropical forest (AMVA-UNAL, 2017). Fig. 1 shows the location and the digital elevation model (DEM) of the basin.

The basin has an area of approximately 0.37 km^2 divided into five surface geological units: fluvio-torrential deposits (Qat), recent landslide deposits (Qdr), debris-flow deposits (QvII), anthropogenic fills (QII), and amphibolites from Medellín (TRmPP). Fig. 2 shows the distribution of the property zones in the basin. Torrential alluvial deposits correspond to materials that are characterized by presenting fresh, mainly subangular, poorly selected blocks within a sandy matrix; recent deposit slip are materials composed of a sandy silt matrix varying from clayey, within which weathered fragments of gneiss and quartz are found which reach sizes up to 10 cm in length; in shed deposits, the clasts range from sub-rounded to subangular, mostly weathered, with sizes ranging from 1 cm to 30 cm in length, the matrix is usually silty-clayey; the composition of the anthropogenic fills is extremely heterogeneous, from homogeneous materials conformed by some technical standards to garbage, organic matter, and simply disposed debris; amphibolites from Medellín are mainly composed of medium-sized hornblende and plagioclase and have a textural variation with grain size from medium (foliated appearance) to fine (massive appearance) (AMVA-UNAL, 2017; SOLINGRAL, 2004; DEACIVIL, 2015).

The topography of the study site was described using a 2 x 2-m digital elevation model (DEM) provided by the Instituto Geográfico Agustín Codazzi (IGAC), with which flow directions and topographic slope maps were generated.

The mechanical properties of the soil were obtained from a geotechnical study (DEACIVIL S.A.S., 2015) developed in an area of approximately 2.3 km2. The basin analyzed in this investigation is within the study area of that geotechnical study. Soil boreholes and different laboratory tests were conducted: natural humidity (128 samples), specific gravity (47 samples), classification tests (113 samples), granulometry (113 samples) and direct shear tests (56 samples).

The soil effective cohesion and internal friction angle were calculated for each geological unit from the results of the direct shear test, and the soil unit weight from the natural humidity and specific gravity tests. The mean values of these soil mechanical parameters were revised comparing with typical values of the literature for the soil types of these geological units and a regional study of landslide hazard assessment accomplished by AMVA and the National University of Colombia (AMVA and Universidad Nacional de Colombia-UNAL 2018) in Envigado and other six

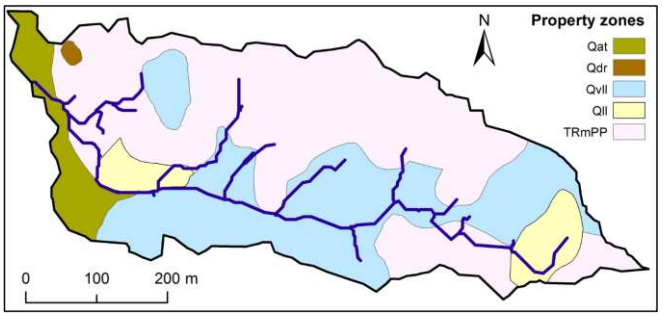

Figure 2. Spatial distribution of the homogeneous geotechnical property zones (geology).

municipalities of the Valle de Aburrá. Table 1 shows the values of these parameters for each geological unit.

Table 1. Values of input parameters for each geological unit.

Parameter	Qat	Qdr	QvII	QII	TRmPP
ϕ' (°)	32	25.09	23.1	30	30
c' (kPa)	5	12.5	18	7.9	10
γ (kN/m^3)	19	15.65	17.85	19	18
K_s (m/s)	5.0 x10^{-5}	1.0 x10^{-7}	1.0 x10^{-6}	1.0 x10^{-8}	5.0 x10^{-8}
θ_s (m^3/m^3)	0.461	0.57	0.601	0.41	0.413
θ_r (m^3/m^3)	0.111	0.278	0.223	0.037	0.149
α (m^{-1})	1	1	1.4	2.5	1.8

The long-term background rainfall rate (I_{ZLT}) is calculated as the average multi-annual precipitation (231 mm) for the historic rainiest month (October) in the Valle de Aburrá, determined in an investigation developed by the AMVA and National University of Colombia (AMVA & UNAL, 2018). I_{ZLT} is defined as a constant value in the entire basin, equivalent to 8.63 * 10^{-8} m/s.

The saturated hydraulic diffusivity (D_0) has been estimated by many authors as a multiple of the hydraulic conductivity (Baum, Godt, & Coe, 2011; Bordoni, Meisina, Valentino, Bittelli, & Chersich, 2015; García-Aristizábal, Aristizábal, Marín, & Guzmán, 2019; Liu & Wu, 2008), between 2 and 500 times K_s. In this research, the relation $D_0 = 100\ K_s$ is adopted, as in different landslide susceptibility analysis using TRIGRS (The Viet, Alvioli, Lee, & An, 2018; Tran The Viet, Lee, An, & Kim, 2017).

The soil thickness is estimated as a function of the slope, based on the soil depth model proposed by Saulnier et al. (1997). It represents the impermeable basal boundary (vertical depth of the lower boundary, d_{lz}). The soil thickness is calculated by equation (10).

$$d_{lz} = z_{max}\left[1 - \frac{\tan\delta - \tan\delta_{min}}{\tan\delta_{max} - \tan\delta_{min}}\left(1 - \frac{z_{min}}{z_{max}}\right)\right], \qquad (10)$$

where z_{min} and z_{max} are the minimum and maximum values of soil thickness, δ is the slope angle, and δ_{min} and δ_{max} are the minimal and maximal values of slope angle. For the five geological units, a value of z_{min} = 0.2 m was assumed, while the z_{max} varied for the amphibolites from Medellín (2 m), debris-flow deposits (3.5 m),

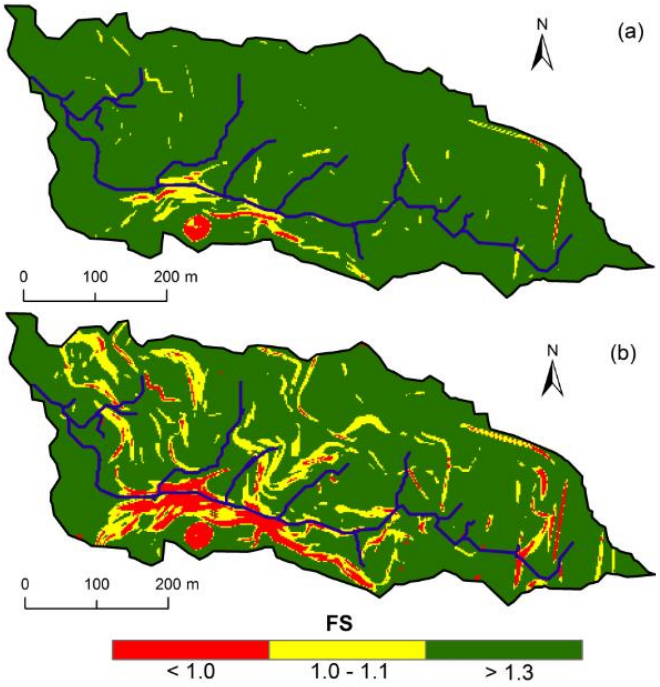

Figure 3. Factor of safety (FS) using Papa et al. (2013) model: (a) before rainfall (dry conditions); (b) groundwater level at the soil surface (saturated conditions).

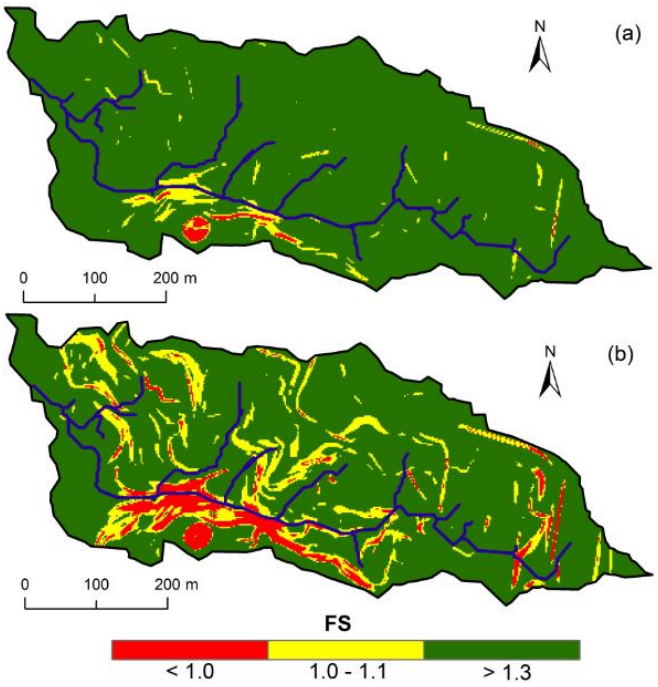

Figure 4. Factor of safety (FS) using TRIGRS: (a) before rainfall (dry conditions); (b) groundwater level at the soil surface (saturated conditions).

recent landslide deposits (3.5 m), anthropogenic fills (3.5 m), and fluvio-torrential deposits (3.5 m). The initial groundwater level is established at the same basal boundary (d_{Lz}), as simulated by different authors using TRIGRS (Kim, Im, Lee,

Hong, & Cha, 2010; Roberto J. Marín & Osorio, 2017b; D. W. Park, Nikhil, & Lee, 2013; Vieira, Fernandes, & Filho, 2010).

In another study site, a few kilometers from the watershed of Envigado (Colombia) implemented in this work, Marín et al. (2019) studied the incidence of the critical failure area (a_c) values used for defining rainfall thresholds using TRIGRS (v2.0). They determined that the rainfall intensity and duration conditions for initiation of shallow landslides in this study site exhibit scaling properties determined by relationships of power-law equations, as was described by Alvioli, Guzzetti, & Rossi (2014) for a different region in Central Italy. In the same study site, Marin & Mattos (2019) carried out three sets of Monte Carlo simulations using TRIGRS to characterize the uncertainty in a landslide susceptibility assessment.

3 RESULTS AND DISCUSSION

Figures 3 and 4 show the factor of safety (FS) in the watershed of Envigado with the Papa et al. (2013) and TRIGRS model, respectively, for dry (Fig. 3a and 4a) and completely saturated conditions (Fig. 3b and 4b). Similar results were obtained using both models. The dry scenario (without rainfall) assumed a water table coincident with the lower boundary and in both cases, a relatively small number of grid cells predicted instability (FS < 1.0, red grid cells in Fig. 3 and 4): 1.0% for the Papa's model and 0.7% for TRIGRS (Figure 5).

The saturated scenario was simulated assuming the water table at the ground surface. Also, the failure area and the spatial distribution of the landslides predicted were similar in both models: 6.4% for Papa's model and 6.1% for TRIGRS (Figure 5).

Figures 6 and 7 show the rainfall thresholds for the study site, using the Papa's and TRIGRS model, respectively, for three different values of critical failure area (a_c): 1%, 2%, and 3%. The position of the rainfall thresholds depends on the a_c values, with a tendency to locate the threshold curve at an upper (and right) part of the graph as a_c increases. It was expected because it means that more extreme rainfall conditions (I-D) are required to cause a greater failing area. Tables 2 and 3 show the equations of the rainfall thresholds constructed.

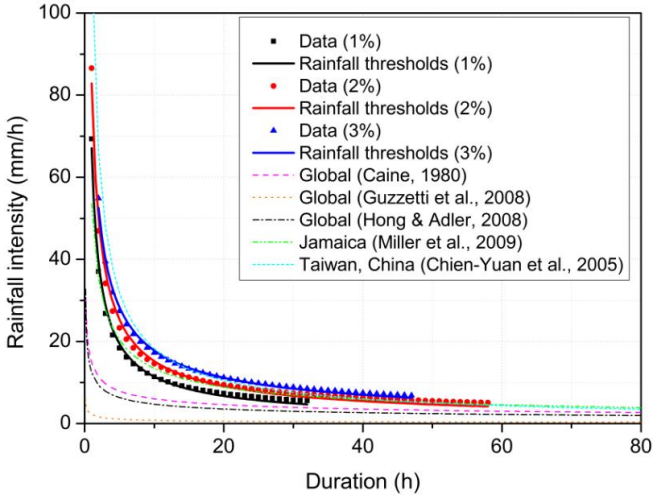

Figure 6. Rainfall thresholds using Papa et al. (2013) for different a_c values. The points (data) represent the critical I-D values calculated in the simulation.

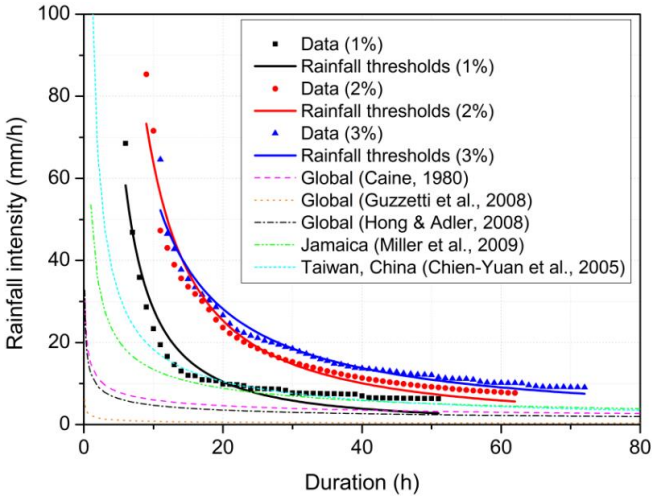

Figure 7. Rainfall thresholds using TRIGRS for different a_c values. The points (data) represent the critical I-D values calculated in the simulation.

Table 2. Equations of rainfall thresholds for different critical area (a_c) percentages in the sub-basin using the Papa's model.

a_c	Equation	R^2	Range of D
1%	$I = 67.08D^{-0.77}$	0.994	1 h ≤ D ≤ 32 h
2%	$I = 82.88D^{-0.74}$	0.992	1 h ≤ D ≤ 58 h
3%	$I = 83.75D^{-0.67}$	0.996	2 h ≤ D ≤ 47 h

Table 3. Equations of rainfall thresholds for different critical area (a_c) percentages in the sub-basin using TRIGRS.

a_c	Equation	R^2	Range of D
1%	$I = 752.73D^{-1.43}$	0.918	6 h ≤ D ≤ 51 h
2%	$I = 1364.02D^{-1.33}$	0.959	9 h ≤ D ≤ 62 h
3%	$I = 620.81D^{-1.03}$	0.965	11 h ≤ D ≤ 72 h

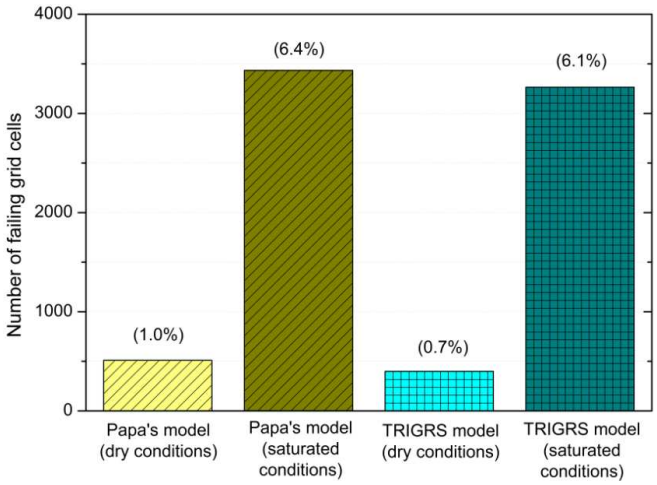

Figure 5. Number of grid cells and failure area for the dry and saturated scenarios, with Papa's and TRIGRS models.

With Papa's model (Fig 6), the slope of the curve (shape parameter β) slightly decreased and the scale parameter (intercept α) increased as a_c increased (Table 2). With TRIGRS (Fig. 7), β also decreased, but the intercept α varied without a regular trend (Table 3). The threshold position also presented a high variation between the curve of a_c = 1% and the others, and great closeness among the latter (a_c = 2% and 3%).

In regression analysis, Pearson's correlation coefficient (R^2) measures the degree of association of two variables. A value of $R^2 = 1$ indicates that there is a perfect positive correlation (i.e., the value of one variable is predicted by taking a certain value from another variable through a direct relationship); on the contrary, $R^2 = 0$ indicates that there is no correspondence between the variables or parameters involved.

The regression models are classified as linear and non-linear. In this study, there is a non-linear relationship based on an exponential function between the rainfall intensity I and duration D (eq. 1). In the Papa et al. (2013) model, a turning point is identified between 8 h and 13 h, approximately, for the three values of a_c, so that (i) before this turning point the intensity increases significantly as the duration decreases, (ii) and after this point the intensity gradually decreases as the duration increases. In the TRIGRS model, the turning point is approximately between 20 h and 25 h for the curves corresponding to ac = 2% and ac = 3%. For ac = 1%, the turning point is around D = 18 h.

These variations in the Papa's model have a certain pattern of uniform differences depending on the proportion of the area of failure, unlike those observed in the diagrams of the TRIGRS model in which there are significant differences in the turning point for a_c = 1% with respect to a_c = 2% and a_c = 3%. It can be possibly explained by the way in that the unsaturated infiltration model of TRIGRS simulates the infiltration process, so that an increase in the rainfall intensity cannot be assumed to be directly related to a percentage of the failure area in a study site. The duration ranges of the thresholds obtained with TRIGRS differs greatly from those with Papa's model. The initial and final durations are greater and increase with a_c (Table 3). On the other hand, with Papa's model, these trends are not evident (Table 2).

All of the rainfall thresholds calculated have a good fit to a power-law curve ($R^2 > 0.9$), but in the Papa et al. (2013) model there is a higher correlation (above 0.99) and a smaller variation in R^2 for the three values of a_c, as shown in Tables 2 and 3.

The rainfall thresholds are represented by an equation that is applicable under a range of durations. In this sense, differences in the results of both models are found. With Papa's model, the first duration simulated (1 h) caused instability over a larger area than the critical values of 1% and 2% (a_c). As none simulation was performed with a rainfall duration lower than 1 h, it is not recommended to assume that the threshold is strictly applicable (or uniquely) for longer durations (than 1 h). This reasoning can be extended for any duration range, with major importance for the initial point of the rainfall threshold. If used in a landslide early warning system, the threshold could be implemented starting from the previous duration in which the first critical I-D point is reached (e.g. 0 h, for the cases of a_c = 1% and 2%).

4 CONCLUSIONS

In this work, a comparison between rainfall thresholds defined by means of two physical-based models for shallow landslides was accomplished. The factor of safety (FS) calculated in each grid cell of the watershed in Envigado (Colombia), using the hydrologic and slope stability models of TRIGRS and Papa et al. (2013), respectively, is used to determine the mean rainfall intensity (I) and rainfall duration (D) conditions that trigger slope failure in a critical failure area (a_c) of the study site. For this, multiple simulations on these models are

required and the critical I-D conditions are adjusted to power-law equations.

The failure area in both dry (assuming water table in the lower boundary) and completely saturated conditions (assuming water table at the ground surface) was similar for the TRIGRS and Papa et al. (2013) models. Nevertheless, the rainfall thresholds obtained with these models differed greatly in the range of durations in which the thresholds are applicable. In TRIGRS, the infiltration model (for unsaturated initial conditions) has an unsaturated zone (above the water table) that absorbs part of the water infiltrated delaying the infiltration at depth. It is more significant for soils with low hydraulic conductivities, as in a great part of the study area. For this, the failure (simulated in TRIGRS) can occur in longer times than in the other model.

The rainfall thresholds determined using both models presented a good fitting to a power-law curve, but the Papa et al. (2013) model had a higher correlation ($R^2 > 0.99$) for the different values of the critical failure area and a smaller variation in R^2. Nevertheless, it is important to mention that the critical I-D conditions obtained from the simulations using a physical model do not necessarily have to be fitted to this equation and the sets of critical I-D values could be used directly as the threshold (e.g. using an interpolation). In any case, future works require validation of the thresholds defined for a specific area before a possible implementation in landslide early warning systems. In this sense, the critical failure area (a_c) for a study site could be determined with a comparison of the performance of rainfall thresholds calculated with different values of a_c.

5 REFERENCES

Alvioli, M., & Baum, R. L. (2016). Parallelization of the TRIGRS model for rainfall-induced landslides using the message passing interface. *Environmental Modelling & Software*, *81*, 122–135. https://doi.org/10.1016/j.envsoft.2016.04.002

Alvioli, M., Guzzetti, F., & Rossi, M. (2014). Scaling properties of rainfall induced landslides predicted by a physically based model. *Geomorphology*, *213*, 38–47. https://doi.org/10.1016/j.geomorph.2013.12.039

Aristizábal, E., & Sánchez, O. (2019). Spatial and temporal patterns and socioeconomic impact of landslides in the tropical and mountainous Colombian Andes. *Disasters*. https://doi.org/https://doi.org/10.1111/disa.12391

Aristizábal, E., Vélez, J. I., Martínez, H. E., & Jaboyedoff, M. (2016). SHIA_Landslide: a distributed conceptual and physically based model to forecast the temporal and spatial occurrence of shallow landslides triggered by rainfall in tropical and mountainous basins. *Landslides*, *13*(3), 497–517. https://doi.org/10.1007/s10346-015-0580-7

Balzano, B., Tarantino, A., Nicotera, M. V., Forte, G., de Falco, M., & Santo, A. (2019). Building physically based models for assessing rainfall-induced shallow landslide hazard at catchment scale: case study of the Sorrento Peninsula (Italy). *Canadian Geotechnical Journal*, *56*(9), 1291–1303. https://doi.org/10.1139/cgj-2017-0611

Baum, R. L., Savage, W. Z., & Godt, J. W. (2002). TRIGRS–a Fortran program for transient rainfall infiltration and grid-based regional slope-stability analysis. USGS Open-File Report 02–0424. *US Geological Survey, Reston, VA*.

Baum, R. L., Savage, W. Z., & Godt, J. W. (2008). *TRIGRS- A Fortran Program for Transient Rainfall Infiltration and Grid-Based Regional Slope-Stability Analysis, Version 2. 0*. U.S. Geological Survey Open-File Report.

Baum, Rex L., Godt, J. W., & Savage, W. Z. (2010). Estimating the timing and location of shallow rainfall-induced landslides using a model for transient, unsaturated infiltration. *Journal of Geophysical Research*, *115*(F3), F03013. https://doi.org/10.1029/2009JF001321

Bogaard, T., & Greco, R. (2018). Invited perspectives: Hydrological perspectives on precipitation intensity-duration thresholds for landslide initiation: proposing hydro-meteorological thresholds. *Natural Hazards and Earth System Sciences*, *18*(1), 31–39. https://doi.org/10.5194/nhess-18-31-2018

Corominas, J., van Westen, C., Frattini, P., Cascini, L., Malet, J.-P., Fotopoulou, S., … Agliardi, F. (2014). Recommendations for the quantitative analysis of landslide risk. *Bulletin of Engineering Geology and the Environment*, *73*(2), 209–263.

Fell, R., Corominas, J., Bonnard, C., Cascini, L., Leroi, E., & Savage, W. Z. (2008). Guidelines for landslide susceptibility, hazard and risk zoning for land-use planning. *Engineering Geology*, *102*(3), 99–111.

García-Aristizábal, E. F., Aristizabal, E. V., Marín, R. J., & Guzman-Martinez, J. C. (2019). Implementación del modelo TRIGRS con análisis de confiabilidad para la evaluación de la amenaza a movimientos en masa superficiales detonados por lluvia. *TecnoLógicas*, *22*(44), 111–129. https://doi.org/10.22430/22565337.1037

Gardner, W. R. (1958). Some steady-state solutions of the unsaturated moisture flow equation with application to evaporation from a water table. *Soil Science*, *85*(4), 228–232. https://doi.org/10.1097/00010694-195804000-00006

Ho, J.-Y., Lee, K. T., Chang, T.-C., Wang, Z.-Y., & Liao, Y.-H. (2012). Influences of spatial distribution of soil thickness on shallow landslide prediction. *Engineering Geology*, *124*, 38–46.

Ip, S. C. Y., Rahardjo, H., & Satyanaga, A. (2020). Three-dimensional slope stability analysis incorporating unsaturated soil properties in Singapore. *Georisk: Assessment and Management of Risk for Engineered Systems and Geohazards*, 1–15. https://doi.org/10.1080/17499518.2020.1737880

Iverson, R. M. (2000). Landslide triggering by rain infiltration. *Water Resources Research*, *36*(7), 1897–1910. https://doi.org/10.1029/2000WR900090

Kim, D., Im, S., Lee, C., & Woo, C. (2013). Modeling the contribution of trees to shallow landslide development in a steep, forested watershed. *Ecological Engineering*, *61*, 658–668. https://doi.org/10.1016/j.ecoleng.2013.05.003

Kim, D., Im, S., Lee, S. H., Hong, Y., & Cha, K.-S. (2010). Predicting the rainfall-triggered landslides in a forested mountain region using TRIGRS model. *Journal of Mountain Science*, *7*(1), 83–91. https://doi.org/10.1007/s11629-010-1072-9

Lanni, C., McDonnell, J., Hopp, L., & Rigon, R. (2013). Simulated effect of soil depth and bedrock topography on near-surface hydrologic response and slope stability. *Earth Surface Processes and Landforms*, *38*(2), 146–159.

Marin, R. J., & Mattos, Á. J. (2019). Physically-based landslide susceptibility analysis using Monte Carlo simulation in a tropical mountain basin. *Georisk: Assessment and Management of Risk for Engineered Systems and Geohazards*, 1–14. https://doi.org/10.1080/17499518.2019.1633582

Marin, R. J., & Velásquez, M. F. (2020). Influence of hydraulic properties on physically modelling slope stability and the definition of rainfall thresholds for shallow landslides. *Geomorphology*, *351*, 106976. https://doi.org/10.1016/j.geomorph.2019.106976

Marín, R.J., & Osorio, J. P. (2016). Evaluation of slope stability quantifying the effect of vegetation. In *2nd International Specialized Conference on Soft Rocks - an ISRM Specialised Conference, ICSR 2016* (Vol. 2016-Janua). International Society for Rock Mechanics.

Marín, Roberto J. (2017). Importancia de la predicción de movimientos en masa en el Valle de Aburrá. *Revista Ingeniería & Sociedad*, *12*(1), 26–31. Retrieved from https://aprendeenlinea.udea.edu.co/revistas/index.php/ingeso/article/view/329516/20785952

Marín, Roberto J., García-Aristizábal, E., & Aristizábal, E. (2019). Umbrales de lluvia para deslizamientos superficiales basados en modelos físicos: aplicación en una subcuenca del Valle de Aburrá (Colombia). *DYNA*, *86*(210), 312–322. https://doi.org/10.15446/dyna.v86n210.77166

Marín, Roberto J., Marín-Londoño, J., & Mattos, Á. J. (2020). Análisis y evaluación del riesgo de deslizamientos superficiales en un terreno montañoso tropical: implementación de modelos físicos simples. *Scientia et Technica*, *25*(1), 164–171.

Marín, Roberto J., & Osorio, J. P. (2017a). Efectos de la vegetación en la estabilidad de laderas: una revisión. *Revista Politécnica*, *13*(24), 113–126.

Marín, Roberto J., & Osorio, J. P. (2017b). Modelación de la contribución arbórea en análisis de susceptibilidad a deslizamientos superficiales. *Revista EIA*, *14*(28), 13–27.

Marín, Roberto J, Guzmán-Martínez, J. C., Martínez Carvajal, H. E., García-Aristizábal, E. F., Cadavid-Arango, J. D., & Agudelo-Vallejo, P. (2018). Evaluación del riesgo de deslizamientos superficiales para proyectos de infraestructura: caso de análisis en vereda El Cabuyal. *Ingeniería y Ciencia*, *14*(27), 153–177. https://doi.org/10.17230/ingciencia.14.27.7

Montgomery, D. R., & Dietrich, W. E. (1994). A physically based model for the topographic control on shallow landsliding. *Water Resources Research*, *30*(4), 1153–1171. https://doi.org/10.1029/93WR02979

Montrasio, L., & Valentino, R. (2008). A model for triggering mechanisms of shallow landslides. *Natural Hazards and Earth System Sciences*, *8*(5), 1149–1159. https://doi.org/10.5194/nhess-8-1149-2008

Moradi, S., Huisman, J., Class, H., & Vereecken, H. (2018). The effect of bedrock topography on timing and location of landslide initiation using the local factor of safety concept. *Water*, *10*(10), 1290.

Papa, M. N., Medina, V., Ciervo, F., & Bateman, A. (2013). Derivation of critical rainfall thresholds for shallow landslides as a tool for debris flow early warning systems. *Hydrology and Earth System Sciences*, *17*(10), 4095–4107. https://doi.org/10.5194/hess-17-4095-2013

Park, D. W., Nikhil, N. V., & Lee, S. R. (2013). Landslide and debris flow susceptibility zonation using TRIGRS for the 2011 Seoul landslide event. *Natural Hazards and Earth System Sciences*, *13*(11), 2833–2849. https://doi.org/10.5194/nhess-13-2833-2013

Park, H. J., Jang, J. Y., & Lee, J. H. (2019). Assessment of rainfall-induced landslide susceptibility at the regional scale using a physically based model and fuzzy-based Monte Carlo simulation. *Landslides*, 1–19.

Richards, L. A. (1931). Capillary conduction of liquids through porous mediums. *Physics*, *1*(5), 318–333. https://doi.org/10.1063/1.1745010

Saulnier, G.-M., Beven, K., & Obled, C. (1997). Including spatially variable effective soil depths in TOPMODEL. *Journal of Hydrology*, *202*(1–4), 158–172. https://doi.org/10.1016/S0022-1694(97)00059-0

Sidle, R. C., & Bogaard, T. A. (2016). Dynamic earth system and ecological controls of rainfall-initiated landslides. *Earth-Science Reviews*.

Srivastava, R., & Yeh, T.-C. J. (1991). Analytical solutions for one-dimensional, transient infiltration toward the water table in homogeneous and layered soils. *Water Resources Research*, *27*(5), 753–762. https://doi.org/10.1029/90WR02772

Taylor, D. W. (1948). Fundamentals of soil mechanics. *Soil Science*, *66*(2), 161.

Vieira, B. C., Fernandes, N. F., & Filho, O. A. (2010). Shallow landslide prediction in the Serra do Mar, São Paulo, Brazil. *Natural Hazards and Earth System Science*, *10*(9), 1829–1837. https://doi.org/10.5194/nhess-10-1829-2010

Zhang, S. J., Xu, C. X., Wei, F. Q., Hu, K. H., Xu, H., Zhao, L. Q., & Zhang, G. P. (2020). A physics-based model to derive rainfall intensity-duration threshold for debris flow. *Geomorphology*, *351*, 106930. https://doi.org/10.1016/j.geomorph.2019.106930

Zhao, B., Dai, Q., Han, D., Dai, H., Mao, J., & Zhuo, L. (2019). Probabilistic thresholds for landslides warning by integrating soil moisture conditions with rainfall thresholds. *Journal of Hydrology*, *574*, 276–287. https://doi.org/10.1016/j.jhydrol.2019.04.062